Thermal Conductivity and Magnon-Phonon Resonant Interaction in Antiferromagnetic $FeCl_2$

G. Laurence and D. Petitgrand

Service d'Electronique Physique, Laboratoire de Physique des Matériaux, Centre d'Etudes Nucléaires de Saclay, 91190 Gif-sur-Yvette, France

(Received 5 February 1973; revised manuscript received 20 April 1973)

The thermal conductivities $K_\perp$ and $K_\parallel$ in the c plane and along the c axis, respectively, have been measured in $FeCl_2$ between 1.2 and 80 °K. Both $K_\perp$ and $K_\parallel$ are found to exhibit, in a wide temperature range, an unusual behavior which reveals the presence of a strong spin-phonon coupling. The experimental results in the antiferromagnetic phase are interpreted on the basis of the magnon-phonon resonant interaction arising from single-ion magnetostriction. It is shown that the thermal conductivity of the resulting magnetoelastic modes can reasonably account for the experimental results: In particular, the anomalous behaviors of $K_\perp$ and $K_\parallel$ between 5 and 17 °K are explained by the effect of a large magnon scattering on the mixed modes. This large scattering leads to a negligible contribution of the spin waves to heat transport. From the $K_\perp$ results, the magnetoelastic coupling constant G_{44} is found to be 3.5 meV.

I. INTRODUCTION

In recent years, several experiments have shown anomalies in the thermal conductivity of magnetic substances.[1-6] Many of these anomalies have been explained either in terms of scattering of phonons by critical fluctuations[7,8] or as a result of magnon-phonon interaction.[9] In the latter case, the contribution of magnons to heat transport has been related to the strength of the magnetoelastic coupling and to the magnitude of the magnon scattering. In a previous paper[10] we have reported the temperature dependence of the thermal conductivity in the c plane of antiferromagnetic $FeCl_2$ and nonmagnetic $CdCl_2$ crystals. For $FeCl_2$, $K_\perp$ results exhibit a pronounced dip shifted to lower temperature comparatively to the Néel point.

The crystal structure of $FeCl_2$ is isomorphous with that of $CdCl_2$, and has an hexagonal layer-type structure. The magnetic properties of $FeCl_2$ have been investigated with a variety of techniques.[11-17] It has been shown that there are a strong ferromagnetic exchange interaction among the intralayer ferrous ions and a weak antiferromagnetic interlayer interaction which gives rise to an antiferromagnetic order up to $T_N = 23.5$ °K. Recently, Birgeneau *et al.*[17] reported a neutron scattering investigation of magnetic excitations in the antiferromagnet $FeCl_2$. On the other hand, the critical behaviors of parallel susceptibility and specific heat of $FeCl_2$[14] and $FeBr_2$[15] have suggested the presence of a large magnetoelastic interaction. Additional evidence for the existence of such an interaction is provided by the effect of pressure[18] and uniaxial strain[19] on magnetic properties, and by the change of lattice constants at the Néel temperature,[20] lately observed.

In Sec. II of this paper, experimental details are given and results of thermal conductivity along the c axis and in the c plane are presented. Section III is devoted to a formulation of the thermal conductivity of $FeCl_2$ in the antiferromagnetic phase. In this section, the calculations of energies and relaxation times of magnetoelastic modes arising from a magnon-phonon resonant interaction are given and the contribution of magnetoelastic modes to thermal conductivity is deduced. In Sec. IV, the experimental results are compared with theory, and the strength of magnetoelastic coupling is deduced. Finally, Sec. V summarizes the main results of the present investigation.

II. EXPERIMENTAL

Experimental Techniques

All measurements were made on single-crystal samples of anhydrous ferrous chloride. To prevent moisture from accumulating, manipulations were carried out in a dry atmosphere. $FeCl_2$ being soft and easily cleaved, it is unable to withstand thermal or mechanical stresses. Precautions must be taken in order to prevent such failures.

The thermal-conductivity measurements between 1.2 and 80 °K were performed, using a steady-state longitudinal-heat-flow method, in a pumped-helium cryostat. The heat flow was, respectively, perpendicular and parallel to the c axis in order to measure $K_\perp$ and $K_\parallel$. In the first case, the sample used was 30-mm long with a cross section of 4.5 $\times$ 5.1 mm and the sample mounting was a conventional one: A heater of ~ 500 Ω was wound on the free end of the specimen, and carbon resistance thermometers (Allen-Bradley) were attached, by means of small copper clamps, at two intermediate positions along the rod.

For $K_\parallel$ measurements, the best sample we got was a 4.4-mm long (c axis) with a cross section of 8 $\times$ 10 mm; such a shape required the unusual as-

sembly shown on Fig. 1. The sample (j) is squeezed between a cryopoint (g) and a warm base (k). To avoid any mechanical overstress in it, 40-μm indium sheets assume a soft thermal contact in each face. The cryopoint is a copper cube, thermally connected to the cryostat by a copper braid (b) and thermocontrolled with a set of heater and thermometer (h). The warm base is composed of a manganin heating coil, wound around a copper rod (l) and rolled into a gold foil used as thermal contact. The effective thermal gradient and the mean temperature are measured with thermometers (i) and (m) which are connected to the sample by small copper wires of 0.5-mm diameter, glued in 0.5-mm holes located in the samples edges at a 3.1-mm pitch. All thermal contacts have been done with GE 7031 varnish or silicon grease, according to the temperature range of experiments. All parts so joined are inserted into a press. The press is composed of two parallel pushers (e) and (o) actuated by nylon rods (f) and belleville washers (c), thus the unavoidable thermal shunt is reduced by using structural material having the lowest thermal conductivity. Most of the loop is of nylon, to reduce contact load changes during measurement, insuring reproducible results. We found that using a simple template made the assembly easier to set up, as the operations around the cryostat in a helium-filled bag were fairly difficult. All leads are of manganin; flanges (d) and (n), their centers, and threaded coupling (a) are of brass. In this arrangement, the accuracy is not limited by temperature measurements or by the thermal shunt but rather by the inaccuracy on temperature sensors positions which can be estimated to ~ 5%. On the other hand, the sample quality seems to be a more determinant factor on the reproducibility from one sample to another; that's why we keep the greatest interest on avoiding to destroy sample during cutting.

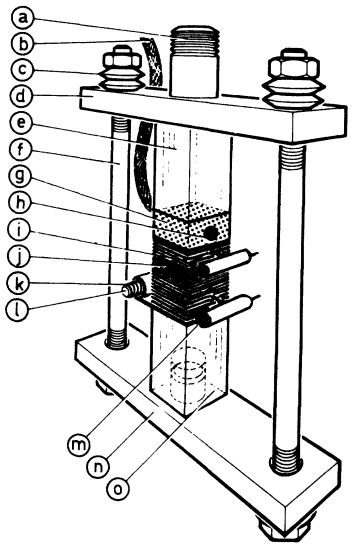

FIG. 1. Holder for thermal-conductivity measurements on a sample having a few mm thickness along the heat-flow direction.

Experimental Results

The most striking feature of thermal-conductivity results (Fig. 2) is the anomalous temperature dependence of $K_\perp$ and $K_\parallel$ between 5 and 40 °K.

The variation of $K_\perp$ as a function of temperature exhibits the following behavior: With increasing temperature, $K_\perp$ increases as $T^{2.7}$ in the interval 1.2–4 °K, reaches a maximum at 5 °K, then between 6 and 17 °K decreases as T^{-2}. After the minimum, at 17 °K, $K_\perp$ increases as T^2 up to about 40 °K, then at higher temperatures exhibits the usual decrease, as in $CdCl_2$.[10]

The conductivity $K_\parallel$ presents a slight dip around 17 °K. At lower temperatures, $K_\parallel$ decreases with decreasing temperature and varies as $T^{2.7}$ below 2 °K. Moreover, the measured values of $K_\parallel$ are smaller than $K_\perp$ values in the whole temperature range 1.2–80 °K.

III. THEORY

In magnetic insulators, two mechanisms are responsible of the spin-phonon coupling[21]: the volume magnetostriction, arising from the phonon modulation of exchange interactions between magnetic ions, and the single-ion magnetostriction due to the modulation of the crystalline field by the motion of the nonmagnetic ions. The first mechanism is quadratic in spin-deviation operators and can contribute to phonon absorption and emission by scattering of spin waves in the ordered phase, as well as critical absorption of phonons near T_N. The effect of this first coupling mechanism on the scattering of phonons near a critical point has been widely investigated.[7,8] In these theories the phonon cross section is expressed as the Fourier transform of four-spin[7] or energy-energy[8] correlation functions which are divergent at T_N (or strongly dependent on $|T - T_N|$). In these two cases of coupling with order parameter and energy density fluctuations, the result is a critical phonon scattering near T_N, which is not observed in the thermal conductivity of $FeCl_2$. The second mechanism yields both quadratic and linear terms in spin-deviation operators. These linear terms are known to give rise, in the ordered phase, to a resonant magnon-phonon interaction which may be described in terms of magnetoelastic excitations.[22]

We shall show in this paper that this magnon-phonon resonant interaction can explain the three main features of the obtained K-versus-T curves: (i) the anomalous behavior of thermal conductivity

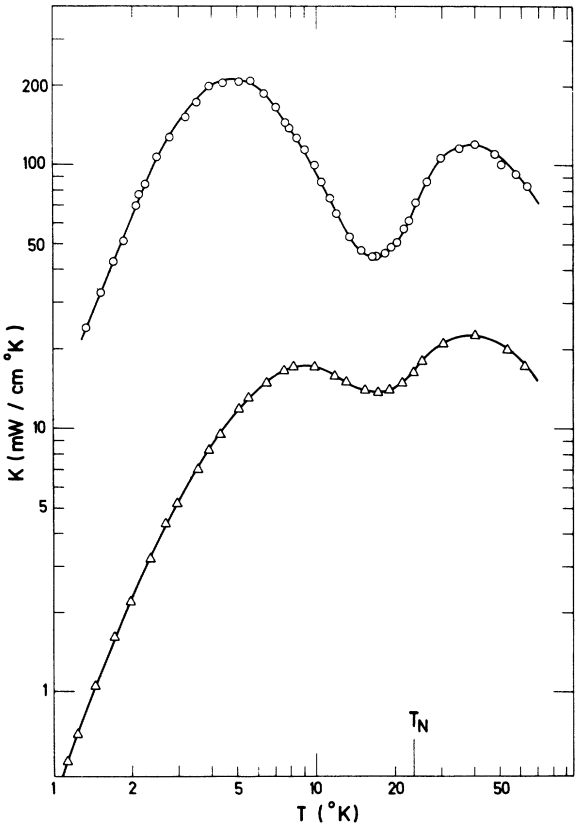

FIG. 2. Variation of the thermal conductivity $K_\perp$ (circles) and $K_\parallel$ (triangles) as a function of temperature.

in a rather large temperature range, particularly at such a low temperature ($T = 5$ °K) that no critical fluctuation can occur; (ii) a minimum of K-versus-T at a temperature ($T \simeq 17$ °K) lower than the Néel temperature ($T_N = 23.5$ °K); (iii) no anomalous behavior close to the Néel temperature.

For this purpose, we shall consider here the effect of the resonant interaction on the thermal conductivity of $FeCl_2$. In order to calculate heat transport by magnetoelastic waves, we shall determine their energy spectra and relaxation times. Thus, we shall first consider the dispersion relations and scattering mechanisms of uncoupled magnons and phonons.

A. Spin Waves

From the $FeCl_2$ spin-wave spectrum determined by Birgeneau *et al.*,[17] we take the following dispersion relations for wave vector $\vec{k}$ perpendicular and parallel to the c axis, respectively:

$$\begin{aligned} \hbar\omega_k &= g\mu_B H_A - 12J_{ab} + 8J_{aa}(1-\cos k\bar{a}), \\ \hbar\omega_k &= g\mu_B H_A - 12J_{ab} \quad \text{for} \quad -\pi/\bar{c} \le k < \pi/\bar{c}, \end{aligned} \tag{1}$$

where

$$\bar{a} = a_0\sqrt{3}/2 \quad \text{and} \quad \bar{c} = 2c_0.$$

a_0 and c_0 are the lattice constants of the conventional hexagonal cell. The values obtained for anisotropy ($g\mu_B H_A = 2$ meV), ferromagnetic intralayer exchange ($2J_{aa} = 0.68$ meV), and antiferromagnetic interlayer exchange ($2J_{ab} = -0.03$ meV) have led to the conclusion that $FeCl_2$ behaves like a two-dimensional ferromagnet rather than an antiferromagnet. We examine now two consequences of such a situation, we shall use later: (a) The Bogoliubov transformation can be approximatively expressed as identity, and (b) intermode four-magnon scattering can be neglected.

1. Ferromagnetic-Magnon Approximation

The spin Hamiltonian of a two-sublattice antiferromagnet is[23]

$$\begin{aligned} \mathcal{H}_{sp} = &-2\sum_{(ll')}{}' J_{aa}\vec{S}^l\vec{S}^{l'} - 2\sum_{(mm')}{}' J_{aa}\vec{S}^m\vec{S}^{m'} \\ &- 2\sum_{(lm)}{}' J_{ab}\vec{S}^l\vec{S}^m - g\mu_B H_A\sum_l S_z^l \\ &+ g\mu_B H_A\sum_m S_z^m, \end{aligned} \tag{2}$$

where S^l and S^m are effective-spin operators ($S = 1$) in sublattices a and b, respectively. Here the primes signify a restriction of the summation to nearest-neighbor pairs.

Introducing the usual spin-wave creation and annihilation operators $a_k^\pm$ and $b_k^\pm$, the spin Hamiltonian becomes

$$\begin{aligned} \mathcal{H}_{sp} = \sum_k [&A_k(a_k^+a_k^- + b_k^+b_k^-) \\ &+ B_k(a_k^+b_k^+ + a_k^-b_k^-)], \end{aligned} \tag{3}$$

with

$$\begin{aligned} A_k = &g\mu_B H_A - 2z_{ab}J_{ab} + J_{aa} \\ &\times\left(1 - 2z_{aa}\sum_{l'}{}' e^{i\vec{k}(\vec{R}_l - \vec{R}_{l'})}\right) \end{aligned} \tag{4}$$

and

$$B_k = -2z_{ab}J_{ab}\sum_m{}' e^{i\vec{k}(\vec{R}_l - \vec{R}_m)}, \tag{5}$$

where $\vec{R}_l$ and $\vec{R}_m$ are the position vectors of lth and mth ions, and z_{aa} and z_{ab} are the numbers of nearest neighbors for ferromagnetic and antiferromagnetic interactions, respectively.

$\mathcal{H}_{sp}$ is diagonalized by the Bogoliubov transformation which involves the new operators $\alpha_k^\pm$ and $\beta_k^\pm$;

$$\begin{aligned} a_k^\pm &= \alpha_k^\pm\cosh\theta_k + \beta_k^\mp\sinh\theta_k, \\ b_k^\pm &= \alpha_k^\mp\sinh\theta_k + \beta_k^\pm\cosh\theta_k, \end{aligned} \tag{6}$$

with

$$\cosh^2\theta_k = [A_k + (A_k^2 - B_k^2)^{1/2}]/2(A_k^2 - B_k^2). \tag{7}$$

In $FeCl_2$,

$$J_{ab} \ll J_{aa} \text{ and } g\mu_B H_A, \tag{8}$$

thus, we have

$$\cosh\theta_k < 1 + \tfrac{1}{2}x^2 \text{ and } \sinh\theta_k < x, \tag{9}$$

with

$$x = -6J_{ab}/(g\mu_B H_A - 12J_{ab}) \simeq 0.04. \tag{10}$$

Then, to a good approximation:

$$\cosh\theta_k \simeq 1 \text{ and } \sinh\theta_k \simeq 0. \tag{11}$$

This approximation will be used in magnon-magnon scattering and magnon-phonon coupling calculations.

2. *Magnon-Magnon Interaction*

The four-magnon part of the Hamiltonian can be written[24]

$$\mathcal{H}_{sp}^{(4)} = \mathcal{H}_{aa}^{(4)} + \mathcal{H}_{bb}^{(4)} + \mathcal{H}_{ab}^{(4)}, \tag{12}$$

where $\mathcal{H}_{aa}^{(4)}$ involves J_{aa} and products such as $a_l^+ a_l^- a_{l'}^+ a_{l'}^-$, $\mathcal{H}_{bb}^{(4)}$ involves J_{aa} and products such as $b_m^+ b_m^- b_{m'}^+ b_{m'}^-$, $\mathcal{H}_{ab}^{(4)}$ involves J_{ab} and products such as $a_l^+ a_l^- b_m^+ b_m^-$; $a_l^\pm$ and $b_m^\pm$ being the usual spin-deviation operators associated to spins $\vec{S}^l$ and $\vec{S}^m$, respectively.

With the aid of the above approximation (11), we have

$$\mathcal{H}_{sp}^{(4)} = \sum_{k_1,k_2,k_3,k_4} \phi_{1,2,3,4} \times [\alpha_{k_1}^+ \alpha_{k_2}^+ \alpha_{k_3}^- \alpha_{k_4}^- + \beta_{k_1}^+ \beta_{k_2}^+ \beta_{k_3}^- \beta_{k_4}^-], \tag{13}$$

where $\phi_{1,2,3,4}$ is a function of $\vec{k}_1$, $\vec{k}_2$, $\vec{k}_3$, $\vec{k}_4$ including the momentum δ function $\delta(\vec{k}_1 + \vec{k}_2 - \vec{k}_3 - \vec{k}_4)$. Thus, the four-magnon scattering which arises from (13) involves only intramode processes.

B. Spin-Wave Scattering

The magnon scattering processes generally taken into account are boundary effect, magnetic defect scattering, magnon-magnon and magnon-phonon scatterings.

The first two processes are known to give rise to a relaxation time,[25]

$$(\tau_k^{mag})^{-1} = v_k^{mag}/L + A_m(k\bar{a})^4, \tag{14}$$

where L is a constant mean free path characterizing boundary-type scattering, A_m is proportional to the density of magnetic defects in the crystal, and v_k^{mag} is the group velocity of magnons.

We shall now consider the relaxation times for normal and umklapp (U) four-magnon processes. The U processes are thought to be important even at temperatures ~ 10 to 20 °K because of the flatness of the spin-wave spectrum. In a first step, we shall derive the mean free path of magnons in normal four-magnon processes. We start with the simplified interaction Hamiltonian (13), so that we are in a ferromagneticlike case. Dyson[26] showed that the cross section for the scattering of two spin waves with wave vectors $\vec{k}_1$ and $\vec{k}_2$ is

$$\sigma_{1,2} \propto \bar{a}^2 (\vec{k}_1 \cdot \vec{k}_2). \tag{15}$$

We obtain the mean free path for scattering of state $\vec{k}_1$ by summing on $\vec{k}_2$:

$$\Lambda_N^{-1}(\vec{k}_1) \propto (k_1\bar{a})^2 \sum_{k_2} (k_2\bar{a})^2 n_{k_2} \cos^2(\vec{k}_1, \vec{k}_2), \tag{16}$$

where n_{k_2} is the Bose distribution for state $\vec{k}_2$. For an isotropic spectrum the density of states is proportional to k_2^2, so that

$$\Lambda_N^{-1}(\vec{k}_1) = l_0^{-1}(k_1\bar{a})^2 \int_0^\pi \frac{(k_2\bar{a})^4}{\exp|\epsilon_{k_2}/k_BT) - 1}\, d(k_2\bar{a}), \tag{17}$$

where l_0 is a characteristic length of four-magnon scattering. In the $FeCl_2$ case, the energy ϵ_{k_2} of state $\vec{k}_2$ may be written, according to (1),

$$\epsilon_{k_2} = \epsilon_0 + \tfrac{1}{2}\epsilon_1[1 - \cos(k_2\bar{a})], \tag{18}$$

which involves a gap ϵ_0 and a spread in energy ϵ_1. The constant l_0 may be determined by considering the limit of (17) for the parabolic dispersion relation considered by Dyson:

$$\epsilon_{k_2} = \tfrac{1}{4}\epsilon_1(k_2\bar{a})^2, \tag{19}$$

where ϵ_1 is related to the J of Dyson by $\epsilon_1 = 4JS$. We obtain in the limit $k_BT \ll \frac{1}{4}\pi^2\epsilon_1$:

$$\Lambda_N^{-1}(\vec{k}_1) = l_0^{-1}(k_1\bar{a})^2 2^4 (k_BT/\epsilon_1)^{5/2}\zeta(\tfrac{5}{2}), \tag{20}$$

where ζ is the Riemann zeta function. By comparison to Dyson's result, we obtain

$$l_0 = 64\pi^{5/2}\bar{a}S^2. \tag{21}$$

Finally, we have

$$\Lambda_N^{-1}(\vec{k}_1) = l_0^{-1}(k_1\bar{a})^2 T^{5/2} F_N(T). \tag{22}$$

$F_N(T)$ is the correction factor to Dyson's formula due to the gap and the nonparabolicity of the dispersion curve:

$$F_N(T) = \int_0^\pi \frac{T^{-5/2}(k_2\bar{a})^4}{\exp(\epsilon_{k_2}/k_BT) - 1}\, d(k_2\bar{a}). \tag{23}$$

For the case of U processes, we shall assume that the result of Dyson (15) remains valid. The only modification is that we can expect to have U processes only for

$$|\vec{k}_1 + \vec{k}_2|\,\bar{a} > \pi.$$

For ease in calculation, we use the condition

$$(k_1 + k_2)\bar{a} > \pi.$$

The umklapp mean free path is then given by

$$\Lambda_U^{-1}(\vec{k}_1) = l_0^{-1}(k_1\bar{a})^2 \times \int_{\pi - k_1\bar{a}}^\pi \frac{(k_2\bar{a})^4}{\exp(\epsilon_{k_2}/k_BT) - 1}\, d(k_2\bar{a}). \tag{24}$$

This can be written

$$\Lambda_U^{-1}(\vec{k}_1) = l_0^{-1}(k_1\bar{a})^2 T^{5/2} F_U(k_1, T), \quad (25)$$

where

$$F_U(k_1, T) = \int_{\pi - k_1\bar{a}}^{\pi} \frac{T^{-5/2}(k_2\bar{a})^4}{\exp(\epsilon_{k_2}/k_B T) - 1}\, d(k_2\bar{a}). \quad (26)$$

Both $F_N(T)$ and $F_U(k, T)$ have been computed numerically.

Lastly, we consider magnon-phonon interaction. The one-magnon–one-phonon process is included in the formalism of magnetoelastic modes, treated later. The scattering of magnons with creation or absorption of a phonon is known to occur only if spin-wave group velocity is greater than the sound velocity v_s.[27] This condition is not satisfied in $FeCl_2$, and processes like $\alpha_k^{\pm}\alpha_{k-q}^{\mp}c_q^{\mp}$ or $\alpha_k^{\pm}\beta_{k-q}^{\mp}c_q^{\mp}$, involving one phonon operator $c_q^{\mp}$, cannot occur. The fusing processes like $\alpha_k^{\pm}\alpha_{q-k}^{\pm}c_q^{\mp}$ can occur but are thought to be effective at too high temperatures to be considered here. Moreover, processes involving more than two magnon and one phonon operators have not been considered here.

To sum up, the combined magnon relaxation time may be written

$$(\tau_k^{\mathrm{mag}})^{-1} = v_k^{\mathrm{mag}}/L + A_m(k\bar{a})^4 + v_k^{\mathrm{mag}} 1_0^{-1}(k\bar{a})^2 T^{5/2} \times [F_N(T) + F_U(k, T)]. \quad (27)$$

C. Phonon Formulation

In this section, we show that the thermal conductivity $K_\perp$ of $FeCl_2$ can be calculated by considering the interaction of the two spin-wave modes with one transverse phonon mode.

For this, we first consider the thermal conductivity of uncoupled phonons. In this case, it is well known that, at low temperature, the dominant contribution to heat flow arises from modes of smaller velocities: for two modes having a sound velocity ratio greater than 3, the contribution of the upper mode can be neglected. For lack of the knowledge of phonon spectrum in $FeCl_2$, we use some results of the Komatsu model[28] for lamellar crystals. For these crystals the three polarization modes (l, t_1, and t_2) of phonons with wave vector perpendicular to the c axis have three different velocities v_l, v_{t_1}, and v_s with $v_l > v_{t_1} > v_s$. In graphite, it was found

$$v_{t_1}/v_s \simeq 21 \quad \text{and} \quad v_l/v_s \simeq 36.$$

This has been related to the fact that the binding energies between atoms in the same layer are much larger than those between atoms in different layers. Such a situation is also known to occur in $FeCl_2$. Thus, we may reasonably assume that the contribution of phonons (l) and (t_1) can be neglected in a nonmagnetic lamellar material.

In the case of a magnetic lamellar material involving magnon-phonon coupling, we assume that the above approximation holds even for coupled modes, namely, the magnetoelastic modes arising from the phonon branches (l) and (t_1) does not contribute to thermal conductivity.

Lastly, it is to be recalled that three mechanisms of phonon scattering are usually considered: boundary effect, mass-difference scattering, and phonon-phonon scattering. They can be taken into account by assuming the following form for phonon relaxation time[29]:

$$(\tau_q^{\mathrm{ph}})^{-1} = v_s/L + A_p\Omega_q^4 + B\Omega_q^2 T^3, \quad (28)$$

where A_p is given by the Klemens relation applied to a compound,[30] L is a characteristic length of the crystal, and B is a phenomenological parameter for three-phonon processes. $\hbar\Omega_q$ is the energy of a phonon with wave vector $\vec{q}$.

D. Magnon-Phonon Coupling in $FeCl_2$

As mentioned above, we consider the interaction of the transverse phonons (t_2) with the two degenerate magnon branches.

The coupling of phonons with spins of one sublattice by the modulation of crystalline field can be described by the Hamiltonian[31]

$$\mathcal{H}_{\mathrm{int}}^a = \sum_l \sum_{\alpha\beta\gamma\delta} G_{\alpha\beta\gamma\delta} S_\alpha^l S_\beta^l \epsilon_{\gamma\delta}^l, \quad (29)$$

where G is the spin-phonon coupling tensor, S^l the spin of lth ion, and ϵ is the local deformation around the lth ion. In the case of a cubic environment[32]:

$$\mathcal{H}_{\mathrm{int}}^a = \sum_l \left(\frac{G_{11}}{2} \sum_\alpha [3(S_\alpha^l)^2 - S(S+1)]\epsilon_{\alpha\alpha} + G_{44} \sum_{\alpha\beta} \epsilon_{\alpha\beta} S_\alpha^l S_\beta^l \right). \quad (30)$$

If we retain only the terms which are linear in spin-deviation operators and consider the coupling with the transverse phonon branch (t_2), we have

$$\mathcal{H}_{\mathrm{int}}^a = \sum_l G_{44} S_x^l S_y^l \epsilon_{xy}^l. \quad (31)$$

We may then expand the $\vec{S}^l$ to the lowest order in deviation operators $a_l^{\pm}$:

$$S_\pm^l = (2S)^{1/2} a_l^{\mp} \quad \text{and} \quad S_z^l = S - a_l^{+} a_l^{-}. \quad (32)$$

Now, the spin-wave operators $a_k^{\pm}$ are introduced:

$$a_l^{\pm} = N^{-1/2} \sum_k a_k^{\pm} e^{\mp i\vec{k}\cdot\vec{R}_l}, \quad (33)$$

where N is the number of unit cells in the crystal. On the other hand, the local deformation can be expanded in phonon creation and annihilation operators $c_q^{\pm}$:

$$\epsilon_{xy}^l = \frac{-i}{N^{1/2}} \sum_q \left(\frac{\hbar}{2M\Omega_q} \right)^{1/2} q_y$$

$$\times(c_q^- e^{i\vec{q}\cdot\vec{R}_l} - c_q^+ e^{-i\vec{q}\cdot\vec{R}_l}), \quad (34)$$

where M is the mass of the unit cell. Thus, the interaction Hamiltonian $\mathcal{H}_{\rm int}^a$ becomes

$$\mathcal{H}_{\rm int}^a = \sum_k D_k (c_k^+ a_k^- + c_k^- a_k^+), \quad (35)$$

with

$$D_k = G_{44} S (2S)^{1/2} (\hbar/2Mv_s\bar{a})^{1/2} (k\bar{a})^{1/2}. \quad (36)$$

Then the Hamiltonian for magnon-phonon coupling in antiferromagnet $FeCl_2$ can be written

$$\mathcal{H}_{\rm int} = \mathcal{H}_{\rm int}^a + \mathcal{H}_{\rm int}^b, \quad (37)$$

where $\mathcal{H}_{\rm int}^b$ is obtained by substituting $b_k^\pm$ to $a_k^\pm$ in (35). With the aid of (6) and (11), $\mathcal{H}_{\rm int}$ can be expressed in terms of magnon operators $\alpha_k^\pm$ and $\beta_k^\pm$:

$$\mathcal{H}_{\rm int} = \sum_k D_k [c_k^+ (\alpha_k^- + \beta_k^-) + c_k^- (\alpha_k^+ + \beta_k^+)]. \quad (38)$$

The total Hamiltonian may now be written

$$\mathcal{H} = \sum_k \{\hbar\Omega_k c_k^+ c_k^- + \hbar\omega_k (\alpha_k^+ \alpha_k^- + \beta_k^+ \beta_k^-) + D_k [c_k^+ (\alpha_k^- + \beta_k^-) + c_k^- (\alpha_k^+ + \beta_k^+)]\}, \quad (39)$$

where ω_k is given by relation (1) and $\Omega_k = v_s k$. $\mathcal{H}$ may be written in the form

$$\mathcal{H} = (c^+ \alpha^+ \beta^+) \cdot (M) \cdot \begin{pmatrix} c^- \\ \alpha^- \\ \beta^- \end{pmatrix}, \quad (40)$$

where

$$(M) = \begin{pmatrix} \hbar\Omega_k & D_k & D_k \\ D_k & \hbar\omega_k & 0 \\ D_k & 0 & \hbar\omega_k \end{pmatrix}. \quad (41)$$

The energies of the coupled modes are given by the eigenvalues of (M) which are

$$\epsilon_{1,k} = \tfrac{1}{2}\hbar(\Omega_k + \omega_k) - \tfrac{1}{2}[\hbar^2(\Omega_k - \omega_k)^2 + 8D_k^2]^{1/2},$$
$$\epsilon_{2,k} = \hbar\omega_k,$$
$$\epsilon_{3,k} = \tfrac{1}{2}\hbar(\Omega_k + \omega_k) + \tfrac{1}{2}[\hbar^2(\Omega_k - \omega_k)^2 + 8D_k^2]^{1/2}. \quad (42)$$

The resulting spectrum for magnetoelastic modes is shown on Fig. 3(b). The operators $\eta_{i,k}^\pm$, which diagonalize $\mathcal{H}$ into the form

$$\mathcal{H} = \sum_{i,k} \epsilon_{i,k} \eta_{i,k}^+ \eta_{i,k}^-, \quad (43)$$

can be deduced from the eigenvectors of (M). We shall note only that

$$\eta_{2,k}^\pm = 2^{-1/2} (\alpha_k^\pm - \beta_k^\pm). \quad (44)$$

Thus, from Eqs. (42) and (44) we deduce that the second mode is totally magnon type.

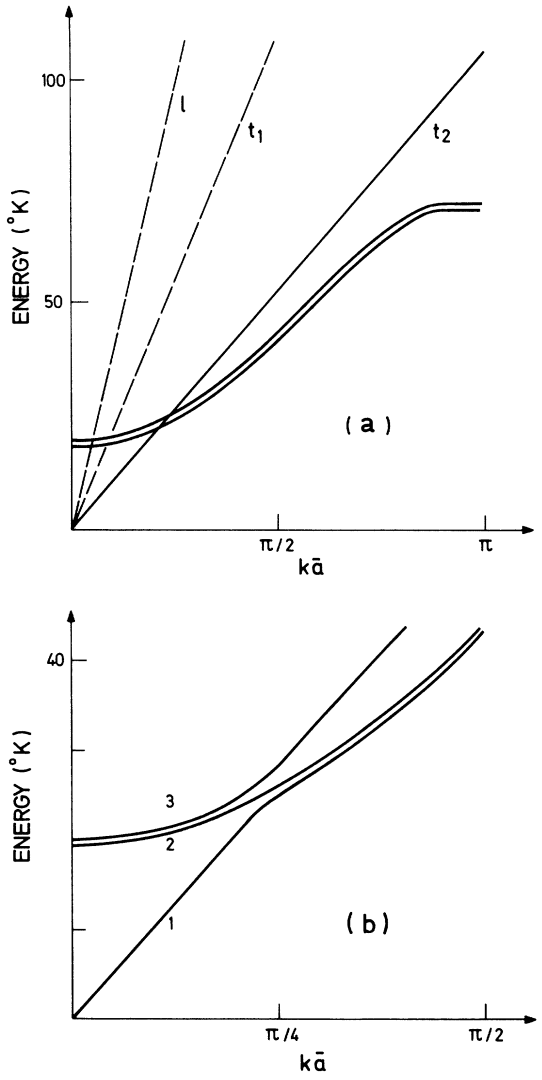

FIG. 3. Dispersion curves in the c plane: (a) for uncoupled phonons and magnons, (b) for magnetoelastic excitations with $G_{44} = 3.5$ meV.

E. Magnetoelastic Wave Scattering and Thermal-Conductivity Formulation

Following the idea of Kittel[22] we take account of the scattering by attributing an imaginary part to the energy of both phonons and magnons:

$$\hbar\tilde{\Omega}_k = \hbar[\Omega_k + i(\tau_k^{\rm ph})^{-1}],$$
$$\hbar\tilde{\omega}_k = \hbar[\omega_k + i(\tau_k^{\rm mag})^{-1}], \quad (45)$$

where $\tau_k^{\rm ph}$ and $\tau_k^{\rm mag}$ are the relaxation times of phonons and magnons, respectively. Replacing Ω_k by $\tilde{\Omega}_k$ and ω_k by $\tilde{\omega}_k$ in (42), we obtain the complex energies for magnetoelastic modes:

$$\tilde{\epsilon}_{i,k} = \epsilon_{i,k} + i\pi_{i,k}. \quad (46)$$

From (46) we deduce the relaxation time of the

magnetoelastic mode (i):

$$\tau_{i,k} = \hbar/\pi_{i,k}. \quad (47)$$

The thermal conductivity of magnetoelastic modes of energies $\epsilon_{i,k}$ and relaxation times $\tau_{i,k}$ is given by[29]

$$K = \frac{4\pi}{3}\frac{1}{(2\pi)^3}\sum_i \int_k v_{i,k}^2 \tau_{i,k} k_B x_{i,k}^2 e^{x_{i,k}} \times (e^{x_{i,k}} - 1)^{-2} k^2 dk, \quad (48)$$

where $i = \{1, 2, 3\}$ is the index of mixed modes, $v_{i,k}$ is the group velocity of mode (i) and $x_{i,k} = \epsilon_{i,k}/k_B T$. The energies $\epsilon_{i,k}$ and relaxation times $\tau_{i,k}$ are, respectively, the real and imaginary parts of the complex energies $\tilde{\epsilon}_{i,k}$ defined by (45)–(47). Equation (48) is equivalent to the simpler Callaway expression[33] for K, which has been shown to be a good approximation when N processes are not dominant. In this case, addition of reciprocal relaxation times includes N and resistive relaxation times as in (27) and (28).

IV. ANALYSIS OF RESULTS AND DISCUSSION

In this section, the experimental results are compared to the calculated thermal conductivity of magnetoelastic waves. As, in $FeCl_2$, spin waves are well defined[17] only up to $0.9\,T_N$, the calculations have been restricted to $T < 21$ °K.

A. Heat Flow Perpendicular to c Axis

The Fig. 4 involves two curves calculated on the basis of the formulation of Sec. III. The curve (a) shows that the general behavior of $K_\perp(T)$ can be described by considering only two scattering mechanisms. The curve (b) is the best fit involving the different scattering mechanisms considered before.

Curve (a). Two scattering mechanisms are taken into account: boundary scattering of phonons and magnons, and four-magnon scattering. The velocity v_s of transverse phonons has been estimated as $\simeq 1.5 \times 10^5$ cm sec^{-1} from lattice-specific-heat data.[34] The value of L is determined from the adjustment of the theoretical curve to the experimental curve at the lowest temperatures ($T < 2$ °K) where the excited modes are purely phonons. The discrepancy between the fitted value $L = 0.02$ cm and the calculated Casimir length $L_C = 0.54$ cm, deduced from the sample cross sections by the relation $L_C = 2\pi^{-1/2} s^{1/2}$, could be related to the presence of cleavage planes perpendicular to the c axis. The mean distance between these planes would thus be approximatively 0.003 cm. The four-magnon scattering constant l_0 and the coupling constant G_{44} are determined by adjusting the computed conductivity in the temperature range $9 < T < 20$ °K where both magnon scattering and magnetoelastic coupling are dominant. However the computed values around 5 °K are greater than the experimental ones.

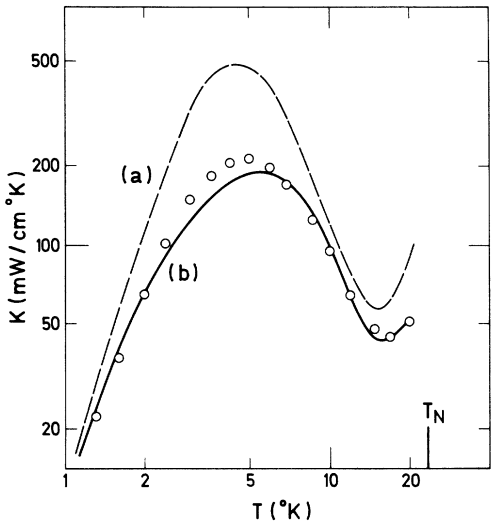

FIG. 4. Comparison of the experimental and calculated thermal conductivity $K_\perp$ in the c plane. Experimental results are the circles. Curve (a) is calculated for a coupling constant $G_{44} = 3.5$ meV, with a boundary parameter $L = 2 \times 10^{-2}$ cm and a magnon-magnon scattering parameter $l_0 = 6 \times 10^{-8}$ cm. Curve (b) includes the parameters of (a) and the scattering process arising from: magnetic-defects ($A_m = 5 \times 10^{10}$ sec^{-1}), mass-difference ($A_p = 5 \times 10^{-43}$ sec^3) and phonon-phonon interaction ($B = 3 \times 10^{-21}$ sec °K^{-3}).

Curve (b). The sharp maximum of curve (a) is the consequence of the strong temperature dependence of the magnon-magnon scattering relaxation times (22) and (26). However, magnetic defects can scatter spin waves even at low temperatures.[25] As $FeCl_2$ is known to contain residual Fe^{++} ions,[35] the relaxation time given by Callaway and Boyd[25] for magnetic defect scattering $[\tau^{-1} = A_m (ka)^4]$ has been introduced in the calculation of curve (b). The value $A_m = 5 \times 10^{10}$ sec^{-1} has been deduced from the fit of $K_\perp$ between 2 and 5 °K. A close agreement between the theoretical curve (b) and experimental points is obtained in the whole temperature range with $G_{44} = 3.5$ meV and $l_0 = 6 \times 10^{-8}$ cm. The above value of l_0 gives a magnon relaxation time (27) $\tau_k^{mag}(k\bar{a} = \pi,\ T = 5\ °K) = 3 \times 10^{-12}$ sec which is in good agreement with the linewidth $\Delta\epsilon(k\bar{a} = \pi,\ T = 5\ °K) = 0.2$ meV obtained in neutron scattering experiments.[17] However, this value is much smaller than the theoretical one given by relation (21): This discrepancy can be related either to the failure of Dyson's theory in the $FeCl_2$ case, or to the existence of some other scattering mechanism. The rather strong value $G_{44} = 3.5$ meV can explain why $FeCl_2$ exhibits one of the largest thermal-conductivity dips in magnetic insulators.

Finally, we have included the mass-difference scattering $[(\tau_q^{ph})^{-1} = A_p \Omega_q^4]$, and the phonon-phonon

scattering $[(\tau_q^{ph})^{-1} = B\Omega_q^2 T^3]$. The value $A_p = 5\times10^{-43}$ sec^3 has been calculated according to Holland, [30] and the value $B = 3\times10^{-21}$ sec °K^{-3} has been deduced from high-temperature thermal-conductivity results in $CdCl_2$, [10] assuming that about 80 °K phonon-phonon interactions are predominant.

B. Heat Flow Parallel to c Axis

Figure 2 shows that the ratio $K_\perp/K_\parallel$ reaches a value of 25 at 1.3 °K. This may be related to a change of transverse phonon velocity or of phonon mean free path. In Komatsu's model related to lamellar structure graphite, transverse phonon velocities for $\vec{q} \perp \vec{c}$ and $\vec{q} \parallel \vec{c}$ are considered as equal. Keeping $v_s = 1.5\times10^5$ cm sec^{-1} for sound velocity, we obtain $L = 6\times10^{-4}$ cm by adjusting calculated and experimental conductivities at 1 °K.

The computed values of thermal conductivity along c axis are shown in Fig. 5. Because of the nearly cubic crystalline field around a ferrous ion, we can consider the magnetoelastic coupling as isotropic and we keep the value $G_{44} = 3.5$ meV for calculation. On the other hand, effective dispersion curves along the c axis are included in the magnetoelastic modes calculation. Keeping the same relaxation times than in heat flow perpendicular to the c-axis case, we obtain a satisfactory agreement between the computed conductivity and experimental results with $L = 6\times10^{-4}$ cm and $A_m = 2\times10^{10}$ sec^{-1}, other parameters involved in $K_\perp$ fit being unchanged. It may be noticed that the value $L \simeq 6\times10^{-4}$ cm was obtained for several samples of various sections and thickness. This is in agreement with the fact that such a low-temperature phonon mean free path is not determined by the external boundaries of the sample.

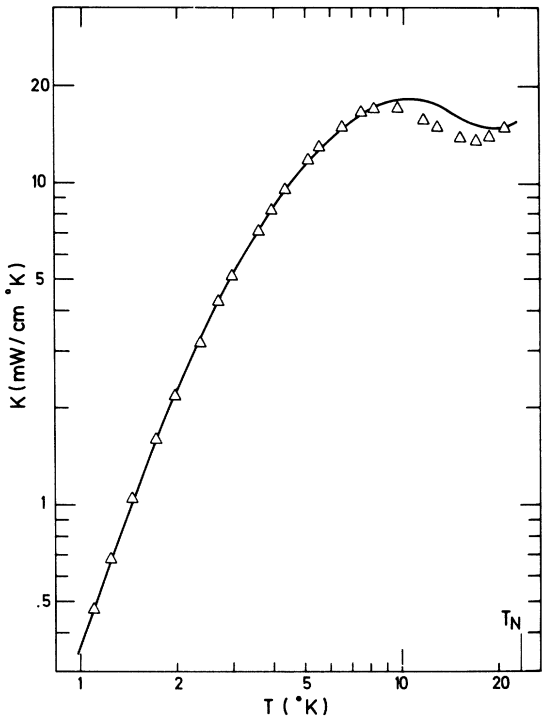

FIG. 5. Comparison of the experimental and calculated thermal conductivity $K_\parallel$ along c axis. Triangles, experimental results; solid line, calculated conductivity obtained for $L = 6\times10^{-4}$ cm and $A_m = 2\times10^{10}$ sec^{-1}, other parameters are unchanged with respect to curve (b) of Fig. 4.

V. CONCLUSION

A magnon-magnon resonant interaction applied to a simplified model founded upon recent results of magnetic properties leads to a reasonable explanation of the anomalous behavior of the thermal conductivity below the Néel temperature in $FeCl_2$. From our experimental results and theory we determine the magnetoelastic coupling constant G_{44}.

The temperatures of maximum (4.5 °K) and minimum (17 °K) of $K_\perp$ in the antiferromagnetic phase can be, respectively, correlated, in this approach with the energies of spin waves at zone center (2.1 meV) and zone boundary (7 meV). For $T < 4.5$ °K, only a purely elastic mode contributes to thermal conductivity which increases as $\sim T^3$. Modes of energy greater than 2.1 meV, having some magnetic character, are excited above 4.5 °K. When the temperature increases, the magnon scattering rapidly increases, decreasing the thermal conductivity of mixed modes. The contribution of the unperturbed magnon mode is then smaller than 2×10^{-3} of the total conductivity in the whole temperature range. For temperatures greater than 17 °K, the upper mode, essentially phononlike, is less scattered than the lower one, essentially magnonlike. Thus, in the interval 17–21 °K the contribution of the upper mode becomes predominant and $K_\perp$ increases. The same explanation, associated to a smaller boundary parameter and a weaker magnon scattering, can account for results of thermal conductivity along the c axis.

ACKNOWLEDGMENTS

The authors express their thanks to Dr. H. J. Albany for his interest in the present work. We are indebted to Dr. D. Walton for stimulating and informative discussions in the initial stages of this work. We would like to thank Professor P. Carrara, Professor J. Joffrin, and A. Bachellerie for useful discussions. We are greatly indebted to O. A. Testard for his technical help in designing and constructing the apparatus. Finally, we wish to thank S. Legrand for supplying $FeCl_2$ crystals, and C. Blanjot for technical assistance.

[1]G. A. Slack, in *Proceedings of the International Conference on Semiconductors, Prague, 1960* (Academic, New York, 1961); Phys. Rev. **122,** 1451 (1961); Phys. Rev. **126,** 427 (1962).
[2]O. Bethoux, P. Thomas, and J. Weil, C.R. Acad. Sci. (Paris) **253,** 2043 (1961).
[3]J. N. Haasbroek and W. J. Huiskamp, Phys. Lett. A 33, 173 (1970); J. N. Haasbroek and A. S. M. Gieske, Phys. Lett. A **31,** 351 (1970); J. N. Haasbroek, thesis (Leiden, 1971) (unpublished).
[4]M. J. Metcalfe and H. M. Rosenberg, J. Phys. C **5,** 450 (1972).
[5]G. S. Dixon and D. Walton, Phys. Rev. **185,** 735 (1969).
[6]J. E. Rives, D. Walton, and G. S. Dixon, J. Appl. Phys. **41,** 1435 (1970); G. S. Dixon, J. E. Rives, and D. Walton, J. Phys. (Paris) **32,** C1-528 (1971).
[7]M. Papoular, J. Phys. (Paris) **28,** Cl-140 (1967); G. E. Laramore and L. P. Kadanoff, Phys. Rev. **187,** 619 (1969).
[8]K. Kawasaki, Prog. Theor. Phys. **29,** 801 (1963); K. Kawasaki, Phys. Lett. A **26,** 543 (1968); H. Stern, J. Phys. Chem. Solids **26,** 153 (1965).
[9]D. Walton, in *International Conference on Phonon Scattering in Solids, Paris, 1972,* edited by H. J. Albany (La Documentation Francaise, Paris, 1972).
[10]G. Laurence, Phys. Lett. A **34,** 308 (1971).
[11]I. S. Jacobs, S. Roberts, and P. E. Lawrence, J. Appl. Phys. **36,** 1197 (1965).
[12]I. S. Jacobs and P. E. Lawrence, Phys. Rev. **164,** 866 (1967).
[13]K. Ono, A. Ito, and T. Fujita, J. Phys. Soc. Jap. **19,** 2119 (1964).
[14]P. Carrara, thesis (Paris, 1968) (unpublished).
[15]M. C. Lanusse, P. Carrara, A. R. Fert, G. Mischler, and J. P. Redoules, J. Phys. (Paris) **33,** 429 (1972).
[16]S. E. Schnatterly and M. Fontana, J. Phys. (Paris) **33,** 691 (1972).
[17]R. J. Birgeneau, W. B. Yelon, E. Cohen, and J. Makovsky, Phys. Rev. B 5, 2607 (1972).
[18]Ch. Vettier (private communication).
[19]J. Hamman and J. A. Nasser, Phys. Status Solidi B **56,** 95 (1973).
[20]R. Kleinberger and J. A. Nasser (private communication).
[21]See, for example, S. K. Ghatak, Phys. Rev. B **5,** 3702 (1972).
[22]C. Kittel, Phys. Rev. **110,** 836 (1958).
[23]F. Keffer, in *Handbuch der Physik*, edited by H. P. J. Wijn (Springer-Verlag, New York, 1966), Vol. XVIII/2.
[24]See Eq. (38.4) of Ref. 23.
[25]J. Callaway and R. Boyd, Phys. Rev. **134,** A1655 (1964).
[26]F. J. Dyson, Phys. Rev. **102,** 1217 (1956).
[27]See Sec. 69 of Ref. 23.
[28]K. Komatsu, J. Phys. Soc. Jap. **10,** 346 (1955).
[29]For a review see P. Carruthers, Rev. Mod. Phys. **33,** 92 (1961).
[30]M. G. Holland, Phys. Rev. **134,** A471 (1964).
[31]R. D. Mattuck and M. W. P. Strandberg, Phys. Rev. **119,** 1204 (1960).
[32]See, for example, M. Boiteux, P. Doussineau, B. Ferry, and U. T. Höchli, Phys. Rev. B **6,** 2752 (1972).
[33]J. Callaway, Phys. Rev. **113,** 1046 (1959).
[34]M. O. Kostryuhova, Zh. Eksp. Teor. Fiz. **46,** 1601 (1964) [Sov. Phys.-JETP **19,** 1084 (1964)].
[35]M. Motokawa and M. Date, J. Phys. Soc. Jap. **23,** 1216 (1967).